Centre for Energy Research
Hungarian Academy of Sciences

A PRACTICAL GUIDE

TO PROMPT GAMMA ACTIVATION ANALYSIS

Authors:

László Szentmiklósi – Zsolt Kasztovszky

Centre for Energy Research, Hungarian Academy of Sciences

2014

BRIEF HISTORY

All activation analytical methods are based on nuclear reactions, in which the atomic nuclei in the sample are excited. By detecting of the emitted radiation qualitative and quantitative analysis is possible. Thanks to their advantages (high selectivity, high sensitivity, non-destructive-, matrix-free- and panoramic features) they are competitive with the more common analytical methods.

The first neutron activation experiment has been performed by GYÖRGY HEVESY and by HILDE LEVI in 1936, just four years after the discovery of neutron (CHADWICK, 1932). Already in the mid-1930s, prompt gamma radiation was incidentally observed when hydrogen-containing material was irradiated by slow neutrons.

Three basic types of neutron activation analysis exist. If the irradiation and the detection of γ-photons are separated in space and time, and only the decay γ-photons are detected, this is the "traditional" **Instrumental Neutron Activation Analysis (INAA)**. In case of **Prompt Gamma Activation Analysis (PGAA)**, the activation and the detection of γ-photons are simultaneous. In case of **Neutron Resonance Capture Analysis (NRCA)**, the analytical signals are originating from resonance-like capture of energetic neutrons into atomic nuclei.

The first PGAA experiment at a research reactor was performed at the Cornell University, US in the 1960s. Although the principles have been already known for some time, it became more widespread only in the 1980s, and was started to be applied as a routine multi-element analytical method since the 1990s.

Until recent times, a crucial limitation of the method was the lack of reliable spectroscopic data. At the turn of the Millennium, significant efforts were made to develop a suitable PGAA spectroscopic library (MOLNÁR, 2004).

At present, around 10 PGAA facilities operate all over the world. Besides Hungary, the most important ones are in Japan, the United States, Germany, South Korea, India and in Argentina. A new instrument is under construction in Morocco, Egypt. The Budapest PGAA laboratory is in operation since 1995.

PRODUCTION AND CLASSIFICATION OF NEUTRONS

Neutron is an chargeless particle with a mass of $1,67492716 \times 10^{-27}$ kg. It can persist only in bound state: as a free particle, the neutron disintegrates into a proton, a β^- (electron) and to an anti-neutrino, with a half-life of 10.24 minutes. Free neutrons can be produced only in **nuclear reactions**. The most common one is the **nuclear fission**; this is a phenomenon in nuclear chain-reactions that happens in nuclear (fission-) reactors (HAHN & STRASSMANN, 1939). There are other neutron sources, such as isotopic sources ^{238}Pu-Be, ^{241}Am-Be and ^{252}Cf), or neutron generators, but they can be less effectively used for PGAA, because of their lower intensities.

Neutrons can be classified according to their energies (Figure 1.). Neutrons, which are in thermal equilibrium with the environment, are referred as **thermal neutrons**. Thermal energy is equivalent to $kT = 25.26$ meV[1] as a characteristic energy at room temperature, or with 2198 m s^{-1} as a most likely velocity. The thermal neutron energies follow Maxwellian distribution. Neutrons having lower energies (~5 meV) are called **cold neutrons**, while those with an energy over 0.1 eV are called **epithermal** ones. Neutrons with energies of MeV order are called **fast neutrons**. However, these threshold limits are not definite; it is more precise, if we differentiate according to energy distribution, i.e. energy spectrum of neutrons. In the epithermal energy range, the energy distribution can be approximated with an $1/E$ function on log-log scale, while fast neutrons show the features of a fissile neutron spectrum, a.k.a. the Watt formula.

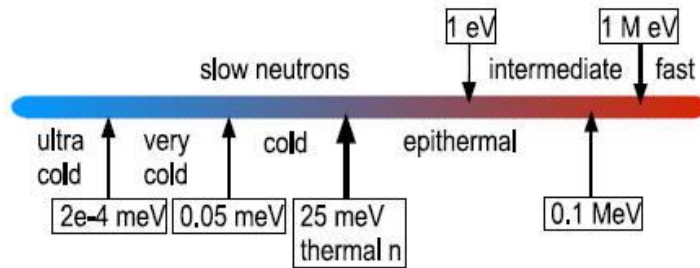---

[1] 1 eV=$1,602\ 176\ 462\ (63) \times 10^{-19}$ J

FIGURE 1: Classification of neutrons according to their energies

In a nuclear fission, fast neutrons are produced, but the probability of the neutron capture is the highest for thermal and for cold neutrons. Therefore, fast neutrons are slowed down by multiple collisions with suitable moderators made of light elements. This process is called thermalisation. At a research reactor, an additional **cold neutron source**, a liquid hydrogen or deuterium containing cell can be applied in order to produce external beam(s) of cold neutrons.

The probability of the interaction between neutrons and the atomic nucleus is characterized by the quantity called **cross-section**; it has the unit of **barn**[2]. In case of cold and thermal neutron capture, the majority of nuclei follow the **1/v-law**. That means that the neutron capture cross-section (σ) is inversely proportional to the velocity of neutrons, i.e. with the square root of neutron energies. In this energy range, σ is easy to calculate from the σ_0 values, a cross-section corresponding to $v_0 = 2200$ m s^{-1} neutron velocity:

$$\sigma = \sigma_0 \frac{v_0}{v} \qquad (1)$$

where $\sigma_0 = \sigma(v_0)$ is the so-called **thermal neutron capture cross-section**. For characterisation of the chemical elements, the average of isotopic cross-sections weighted by isotopic abundances (θ) is used:

$$\sigma = \sum_i \theta_i \, \sigma_i \qquad (2)$$

MAIN FEATURES OF PGAA

- PGAA is based on the **radiative neutron capture**. Based on the energy and intensity of the **γ-radiation** arising from the reaction one can determine the exact composition of an unknown sample. Neutron capture occurs on every nucleus except ^{4}He, thus the method is in principle applicable for the simultaneous **determination of every chemical element**.
- Typically well measurable are some light elements (H, B, Cl, S), heavy metals with environmental significance (Cd, Hg), and some rare earth elements important in geochemistry (Nd, Sm, Gd, Eu).
- PGAA is suitable for **panoramic analysis**, i.e. when the concentration or detection limits of every component in an unknown sample are determined at once.
- The most important advantage of PGAA is the **simple or negligible sample preparation**. In most cases, solid or liquid samples packed in Teflon foil or in Teflon vial are irradiated. Self-supporting samples (e.g. rocks) can even be investigated without packaging.

---

[2] 1 barn = 10^{-28} m^2

- During the analysis, the number of transmuted nuclei is much less than those in case of INAA, thus the isotopic composition is practically not affected (no burn-up effect) and the induced radioactivity is negligible in most cases. Consequently, the method is considered as **absolutely non-destructive** and suitable to study valuable or unique samples.
- The energies and intensities of the emitted photons are determined exclusively by nuclear parameters, and thus are independent of chemical environment of the samples. Therefore, in most cases, PGAA is considered to be **matrix-free**.
- Incoming neutrons and the emitted gamma photons can penetrate through thick layers, therefore PGAA – contrary to many other analytical methods – provides the **average bulk composition of the irradiated and observed volume**. With the help of collimated neutron beam, elemental distribution in an inhomogeneous sample can be determined, too.
- **Detection limits** vary within a wide range from one element to another, and usually, they are significantly higher than those of INAA or of ICP-MS. The best detectable elements can be measured at 0.1 ppm level, while those with low neutron capture cross-sections can be quantified only if they are major components.
- PGAA has a **broad dynamic range**. It means that from the minimum detectable amount of element A in B and from the minimum detectable amount of element B in A, the A/B ratio can vary within an order of 6 to 8. This interval may not be symmetric.
- The uncertainty budget of the measurement and of the evaluation can be rigorously described with statistical methods, and thus the uncertainty of a single measurement can be estimated with a high confidence. The intensity of signals (i.e. the count rate or counts per unit time) from prompt-γ photons is constant, thus **the accuracy of the results can be improved with increasing acquisition time**.
- The PGAA method does not require standardisation measurements for each sample types, a common nuclear data library is suitable for all kinds of samples.
- On the other hand, PGAA is not competitive with other analytical methods, from the points of effectiveness, costs and simplicity.

How is the analytical signal produced in PGAA?

When a slow neutron is captured, a **compound nucleus** is formed first. The excitation energy of the compound nucleus is equivalent to the binding energy of the neutron (7–9 MeV), as the kinetic energy of the neutron is negligible. The compound nucleus can decay through various de-exitation channels, followed by the emission of γ-photons or charged particles.

So, the primary source of the analytical signal is the radiative neutron capture, with other words, the (n,γ)-reaction. During the (n,γ)-reaction, the daughter nucleus emits prompt **γ-photons**, starting from the capture state and in one or several steps it reaches the ground state ($\gamma_1 \ldots \gamma_5$, FIGURE 2a-2b.). The energies and intensities of the γ-photons are characteristic to the de-exitation of the daughter nucleus of ($A+1$) mass number, and thus indirectly to the parent nucleus. This nuclear reaction takes place mostly within 10^{-12} s, that's why the reaction called "prompt". When the $\left({}^{A+1}_{Z}X \right)$ daughter nucleus is stable, the reaction ends with the emission of prompt-γ photons. However, in some cases **radioactive** daughter nucleus is produced that transforms further to a stable one – mostly emitting β^- particle with a definitive $T_{1/2}$ half-life. In much less cases, β^+-decay or electron-capture may occur. During PGAA, both prompt- and **decay-γ photons** (γ_6 on FIGURE 2b.) are detected and can be utilised in the analysis.
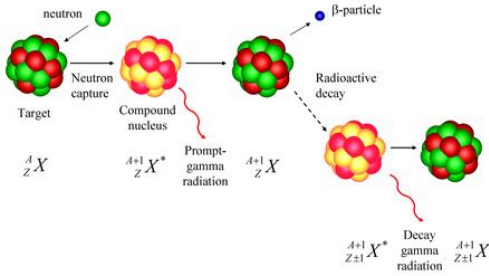
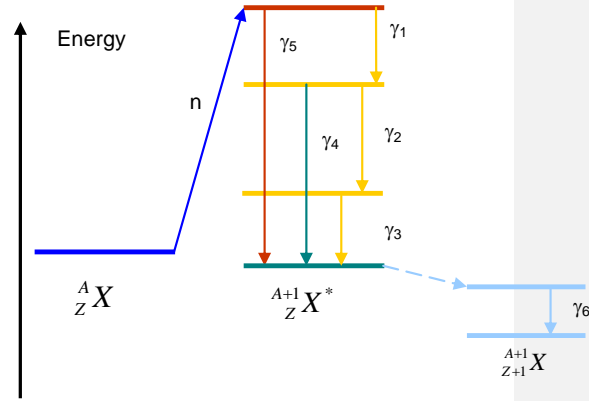**FIGURE 2a.** the origin of the analytical signal in PGAA

FIGURE 2b. The level scheme of radiative neutron capture and a subsequent β^--decay

Quantitative analysis

The number of the emitted prompt-γ photons relative to the number of neutron captures gives the quantity called **emission probability** (P_γ). This emission probability multiplied by the neutron capture cross-section and by the isotopic abundance (θ) is the **partial gamma-ray production cross-section** (σ_γ), a compound nuclear quantity of the fundamental importance in PGAA.

$$\sigma_\gamma = \sigma_0 \, P_\gamma \, \theta \tag{3}$$

The basis of the quantitative analysis is that the **count rate** $\left(\dfrac{dN_P}{dt}\right)$ **of a peak with E_γ energy is proportional to the number of atoms emitting γ-photons of the given energy**. In general, a sample with volume V, irradiated with a neutron beam, will produce a count rate of:

$$\frac{dN_P}{dt} = \int\limits_{V} \int\limits_{E_n=0}^{\infty} \frac{\mu(\mathbf{r}) N_{Av}}{M} \sigma_\gamma(E_n) \, \Phi'(E_n,\mathbf{r}) \, \varepsilon'(E_\gamma,\mathbf{r}) \, dE_n d\mathbf{r} \tag{4}$$

in an E_γ peak, where N_P is the peak area, $\mu(\mathbf{r})$ is the mass density of the examined element as a function of position vector $\mathbf{r}$ in the sample, N_{Av} is the Avogadro number, M is the relative atomic mass of the element, $\Phi'(E_n,\mathbf{r})$ is the neutron flux as a function of neutron energy and the position $\mathbf{r}$ within the sample, $\varepsilon'(E_\gamma,\mathbf{r})$ is the counting efficiency of the detector. With the help of these position-dependent quantities, the inhomogeneous composition of the sample, the spatial inhomogeneity of neutron beam intensity, as well as the gamma absorption and other geometric effects can be in principle taken into account. The general equation (4), however, can be simplified in most practical cases, as follows:

- With proper design of the equipment, the position dependence of the detector efficiency can be minimized,
- Self-shielding and self-absorption in the sample can be taken into account with the help of correction factors,
- In case of small and thin samples, the effect originated from the inhomogeneity of the neutron beam is negligible,
- In case of homogeneous samples, volumetric integral of the density function is replaced by the mass of the sample,

- Regarding the dependence of reaction rates from neutron velocity, a convention is introduced:

The neutron capture cross-sections are calculated as equivalent to monochromatic neutrons with 2200 m s^{-1} (σ_0), according to equation (1) (supposing the validity of $1/v$ law). **Thermal equivalent flux** (Φ_0) is defined so as that the product of the two would give the observed reaction rate:

$$R \equiv N \int_{E_n=0}^{\infty} \Phi(E_n) \cdot \sigma(E_n) \ dE_n = N \int_{E_n=0}^{\infty} v \cdot n(E_n) \cdot \frac{\sigma_0 v_0}{v} \ dE_n =$$
$$= N \cdot \sigma_0 \int_{E_n=0}^{\infty} v_0 \cdot n(E_n) \ dE_n = N \cdot \sigma_0 \cdot \Phi_0 \tag{5}$$

where n is the neutron density, N is the number of atoms in the beam.

As a result of the above simplifications, the counts in one single peak (N_P), collected in t_m time can be calculated as follows:

$$N_P = m \, S \, t_m = \frac{m N_{Av}}{M} \Phi_0 \sigma_\gamma \varepsilon(E_\gamma) t_m \tag{6}$$

where m is the mass of a given element in the sample, S is the analytical sensitivity (cps mg^{-1}).

When ratios of peak areas are studied and concentrations are calculated, the above described effects concern every component. Therefore, many sources of uncertainties, for instance the actual value of neutron flux, can be eliminated.

When the produced nucleus is radioactive, decay-γ photons are also utilised in the analysis. (γ_6 photon on FIGURE 2b.). In this case, it must be taken into account that the count-rates for decay peaks varies in time: it approximates the saturation value of $m \cdot S$ during the neutron irradiation.

ANALYTICAL APPLICATIONS OF PGAA

Applications of PGAA are discussed in many works (ALFASSI 1995, MOLNÁR 2004). The main areas of applications are the following.

- Together with other (radio)analytical methods, PGAA is often used for **quality assurance** of standard reference materials and for **certification** in environmental chemistry and industry.

- **Some industrial applications** are the investigations of metals (hydrogen cells, alloys), impurities in semiconductors, analysis of borosilicate glass, control of heavy metal emission in power plants, as well as analysis of fossil fuels.

- In the **nuclear technology**, analysis of reactor graphite and beryllium, study of reactor poisons, analysis of fuel rods and water from primary cooling loop has been carried out.

- Composition of **foods**, plants and seeds were determined; moreover, **biological**, medical (BNCT) and physiological investigation were carried out. The boron, which has an important role in the growth of the plants and the Ca-metabolism of living organisms, could easily be measurable in matrices containing H, C, N, O and S.

- Exploiting the non-destructive feature of PGAA, various **archaeological** and other **cultural-heritage** related objects (stones, pottery, metal, glass, precious stone, etc.) are studied.

- In **geology, environmental science and cosmo-chemistry,** various rocks, meteorites, etc. can be studied, based on their major and trace components.

- PGAA is perfectly applicable to investigate the composition of various **catalysts**, when small amounts of analytes are available, even under the operation conditions (*in situ*)

- Other applications in **material sciences**: cements, amorphous alloys, fullerene, nanotubes, etc.

THE BUDAPEST PGAA INSTRUMENT

The Budapest Research Reactor and the neutron guides

The Budapest Research Reactor (BRR) is a WWR-SM type light water-type reactor. The reactor has a thermal power of 10 MW; the thermal neutron flux in the core can be as high as 2.2×10^{14} cm^{-2} s^{-1}. The reactor operates in 10-days long campaigns, about 3000 hours per year.

The **cold neutron source** is built in to the tangential channel No. 10. This is a 400 cm^3 volume cell, placed close to the beryllium reflector and filled with liquefied hydrogen. From the cold source, the neutrons are transported to the various experimental stations by neutron guides. The PGAA station is situated about 33 m away from the Reactor (FIGURE 3a.). At the end of this guide, the neutron beam is split into two parts to serve two independent stations: on the upper beam, the **PGAA** (*Prompt-Gamma Activation Analysis*) instrument, while on the lower beam, the **NIPS-NORMA** (*Neutron-Induced Prompt-Gamma Spectrometry*) instrument is operated.

THERMAL NEUTRON INSTRUMENTS:
RAD: DYNAMIC N/GAMMA & STATIC RADIOGRAPHY
BIO: PORT USED FOR BIOLOGICAL IRRADIATION
MTEST: MATERIAL TESTING DIFFRACTOMETER
TAST: TRIPLE AXIS SPECTROMETER
PSD: POWDER DIFFRACTOMETER
TOF: TIME-OF-FLIGHT DIFFRACTOMETER

COLD NEUTRON INSTRUMENTS:
GINA: POLARIZED NEUTRON REFLECTOMETER
IMBS: IN-BEAM MÖSSBAUER SPECTROMETER
SANS: SMALL ANGEL SCATTERING SPECTROMETER
PGAA: PROMPT GAMMA ACTIVATION ANALYSIS
NIPS: NEUTRON INDUCED PROMPT GAMMA SPECTROMETER
REF: REFLECTOMETER
ATHOS: TRIPLE AXIS SPECTROMETER

FIGURE 3a. Top view of the Budapest Research Reactor, the Neutron Guide Hall and the PGAA and NIPS-NORMA experimental stations

The PGAA instrument

The central part of the PGAA instrument is a **HPGe detector**. In our setup this central detector is surrounded by bismuth-**germanate** (*BGO*) scintillator annulus segmented in 8 parts. The so-called "cold finger" and two more „*catcher*" detectors are placed to its rear side. When the γ-photons, which scattered out from the germanium crystal, are absorbed by one of the BGO's segments or by the catchers, the scintillations are detected by photomultiplier tubes. Summing up the scintillation signals, the so-called **Compton-suppressed** detection

6

mode is implemented: signals of the HPGe detector that coincide in time with signals in any scintillator segments are selectively rejected by an **anti-coincidence** gating. This way, single escape peaks are reduced by a factor of 5, double escape peaks are reduced by a factor of 100, and the Compton-plateau is suppressed by a factor of 5–40, while keeping the useful full-energy peak areas. The first two effects simplify the spectrum, while the Compton-suppression improves the detection limits and decreases the counting uncertainties of the peak areas. The detector assemblage is surrounded with a 10 cm thick **lead shielding,** i.e. the γ-photons can reach the HPGe detector only through a narrow lead **collimator**. This arrangement limits the solid angle of the detector, and ensures that γ-photons cannot interact directly with BGO, only after being scattered out from HPGe crystal.
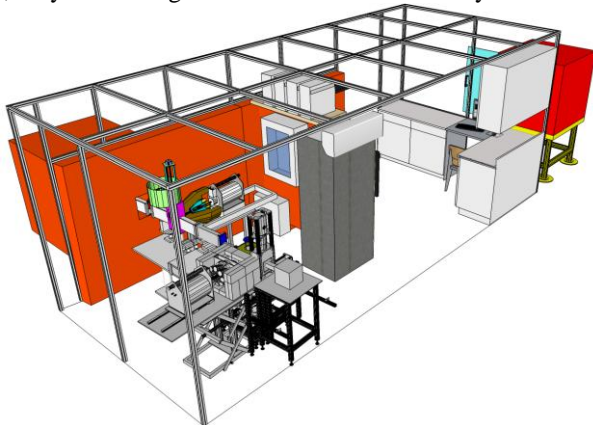

FIGURE 3b. 3D view of the PGAA and the NIPS experimental stations

Main characteristics of the detector system
A) Efficiency

One of the most significant parameters of a γ-detector is the **absolute detection efficiency**, defined as the ratio between the number of detected "events" in the full energy peak and the number of given energy photons emitted from the radiation source. The efficiency curve can be well described with a 6 to 8 order polynomial on log-log scale (FIGURE 4a.).
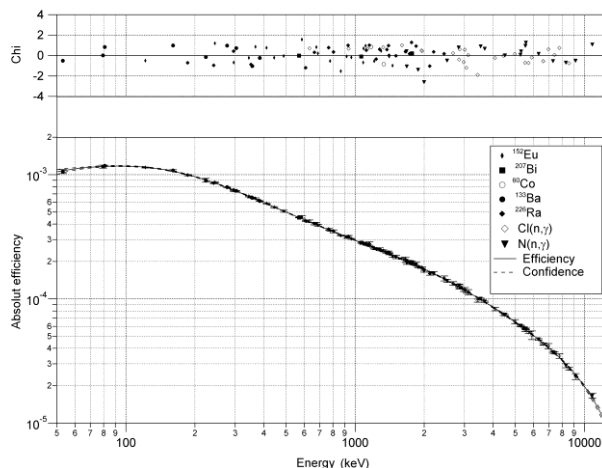

FIGURE 4a. Absolute efficiency of the Budapest PGAA system

Comment [Sz.L.1]: van ilyen ábra angolul

7

B) Nonlinearity

The γ-photons create electron-hole pairs in the sensitive volume of the semiconductor material. Since only about 1.7 eV is transferred during a single interaction, a photon of a few MeV can produce a large number of pairs of positive and negative charges. As the steps of signal detection and processing are basically linear, there is a principal linear correspondence between channel numbers and the energies. In practice, the linearity is not perfect mainly due to the analogue-digital converter (ADC). The systematic deviation from linearity is in the order of 0.1% and can be characterized by the **differential nonlinearity**. In the wide energy range of PGAA, 1–2 channel shift can result in about 1 keV energy bias, which leads to false peak identification; therefore nonlinearity must be taken into correction. According to our experiences, there is only a slow change in the nonlinearity function during a few months period. It means that **nonlinearity calibration,** along with the efficiency measurements, must be regularly repeated. In this procedure, radioactive sources with known γ-energies are measured and the peak positions are compared to their literature energies. A polynomial function is fitted on the data set, and the obtained nonlinearity function is used for correction during the spectrum evaluation stage (FIGURE 4b.).
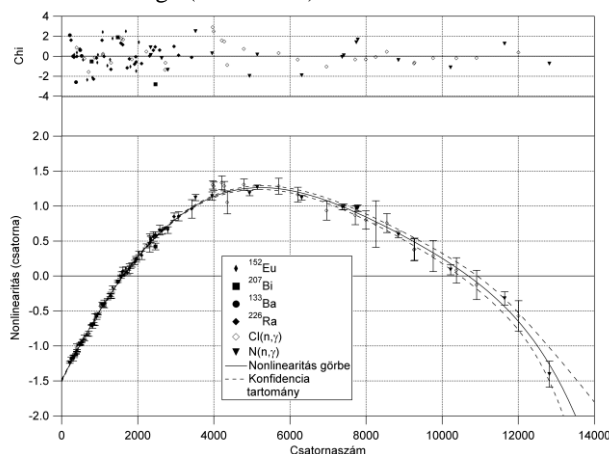

FIGURE 4b. Nonlinearity of the Budapest PGAA system

C) Energy resolution

The other important factor in PGAA is the **energy resolution of the detector**. It can be characterised by the *full width at half maximum* (*FWHM*) of known γ-lines. In case of 1332 keV line of ^{60}Co, FWHM is about 1.8–2.2 keV.

The energy resolution of the spectrometer is determined by the characteristics of the detector and the associated electronics. As a function of energy, the overall peak broadening effect can be calculated in quadrature from contributions of the electronics, the statistical fluctuation of charge creation and the imperfect charge collection.

Calibration of the detector system

In order to determine the above discussed calibration functions, we use γ-sources of accurately known energies and intensities, which cover the whole energy range used in PGAA. At low energy, commercial **radioactive sources** (^{152}Eu, ^{207}Bi, ^{60}Co, ^{133}Ba, ^{226}Ra) are used, while for the 2–11 MeV region **prompt-γ lines of** N and Cl are measured. For the

determination of absolute efficiency curve, the absolute activity of the most precisely calibrated radioactive source is used, and the rest are normalised to this.

The EFFICIENCY, NONLINEARITY and FWHM ANALYSIS modules of the HYPERMET-PC software are used for such calculations.

The signal processing

The first step of signal processing is done by the **preamplifier**. Our RC-feedback type preamplifier creates an exponential pulse with 100–200 ns rise time and a decay constant of 45 μs for each detected event. The further steps of the signal processing are to transform this long pulse to a shorter one, and to derive a quantity still proportional to the original amplitude, which is proportional to the charge created (and therefore to the deposited energy) in the sensitive volume of the detector.

For this purpose **analog** spectroscopic amplifiers were in use for several decades. These units filter and amplify the exponential signal and form them to a semi-Gaussian shape. The amplitude of the semi-Gaussian is read by an analog-digital converter (ADC) and the event is placed to the appropriate channel of a multichannel analyser (MCA). The digitization step is here is at the end of the signal processing chain.

Some years ago a new generation of electronics was commercialized that rely on **digital signal processing**. Here a sampling ADC digitizes already the incoming detector signal and the signal processing is carried out on the numerical data stream by mathematical algorithms. This approach has certain advantages and drawbacks over the conventional systems.
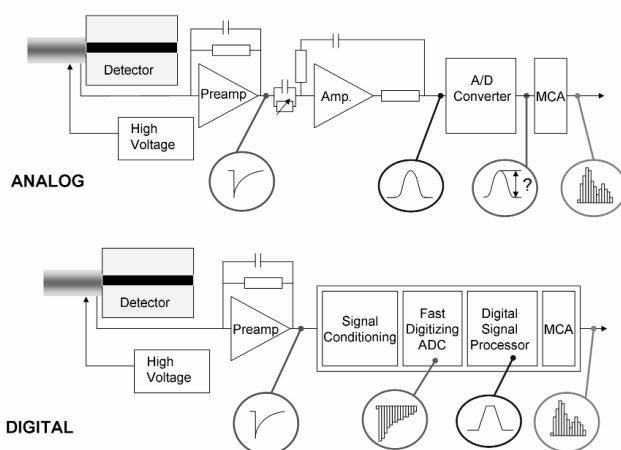

FIGURE 5. Block diagram of analogue and digital signal processing

STEPS OF THE ROUTINE ANALYSIS

Sample preparation and data acquisition

Sample preparation for prompt-γ activation analysis is very simple. Depending on the composition, approximately 0.5–2 g of sample is necessary, which can be solid or liquid. When it is allowed, inhomogeneous and rough samples are powdered and homogenised, then packed into FEP- (fluor ethylene-propylene) bags. The typical dimensions of such filled bags are 20×30 mm^2, while the thickness is about 1–3 mm. Self-supporting samples can be directly mounted by Teflon monofilament strings into the beam. Pellets can be pressed from powder

samples if needed. Liquid samples are irradiated in Teflon vials. Teflon and FEP are favourable, because they do not contribute to the spectrum significantly, and they are chemically resistant.

After packaging, sample is mounted on an aluminium frame to ensure the reproducible positioning, and the frame is placed into the neutron beam. We open the beam shutter, and start the **prompt-γ counting** with the BUDAPEST PGAA DAQ acquisition software (FIGURE 6.). In practice the acquisition time needed can vary within a very wide range, depending on the elements to be identified. According to our experiences, in most cases 30 to 120 minutes are enough to quantify major components in a 1-g geological sample. (In many practical cases, we analyse geological samples: rocks, sediments, soils, minerals. Furthermore, glass or ceramics are very similar to geological samples in composition.) When small amount of sample is available, or detection of a low sensitivity element is requested, acquisition can take up to several days.

When sufficient events have been collected, we save the spectrum and close the beam. For further data treatment, the GENIE 2000 format spectrum with *.CNF extension is converted to S100 format file with *.MCA extension.

Following the experiment, the samples are stored behind lead shielding for a few days, in order to let the **induced radioactivity decay below the exemption level**. After that, the sample can be **returned** to the owner **or sent to further analysis**.
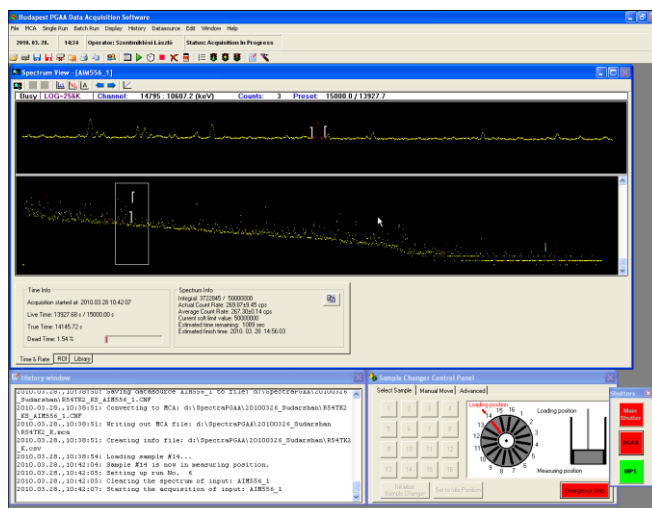

FIGURE 6. Screenshot of the BUDAPEST PGAA DAQ acquisition software

The spectrum evaluation

The useful spectroscopic information is carried by the full-energy peak positions and by the peak areas. The main goal is to determine these quantities as precisely as possible. A typical PGAA spectrum usually consists of hundreds of peaks. For the evaluation, we divide the spectrum to **regions**, each containing up to ten peaks.

For routine spectrum evaluation, HYPERMET-PC is adequate software. At the beginning, a well-known low-energy and a high-energy peak are chosen for **energy and FWHM calibrations**. Then, the software automatically searches and finds the peaks throughout the whole spectrum, sets up the optimal limits of the regions, and fits the model function in each region to the measured histogram values (see Appendix). As a result, an output peaklist with the peak energies, areas and their uncertainties is generated. Finally, the result of the

automatic fit must be revised, and if necessary, corrected observing the residuals and χ^2 values. In many cases, the fit must be improved by modification of the fit parameters or by adding or deleting peaks in the given region.

The FIGURE 7 demonstrates a typical fit by HYPERMET-PC. The so called "step function is well visible under the asymmetric peaks. When the fit of a spectrum is finished, prepared **efficiency and nonlinearity corrections** are loaded, and a final PKL **peaklist** is generated that contains the peak positions, energies, FWHMs, areas, and their estimated uncertainties, as well as χ^2 of the fit for every peak.
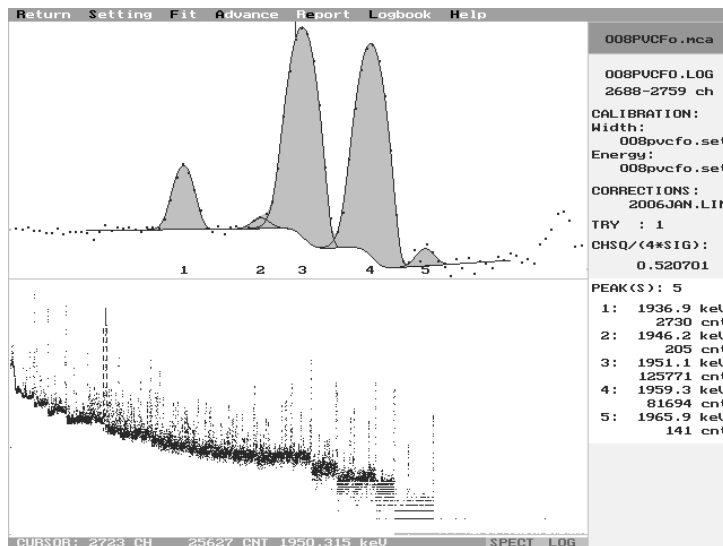

FIGURE 7. The fit of a chlorine doublet with HYPERMET-PC.

Calculation of the elemental composition

The calculation of the elemental composition is done by a MICROSOFT EXCEL **macro** (FIGURE 8.), which requires the peaklist from HYPERMET-PC as an input. Steps like identification of prompt-γ peaks, comparison with the PGAA library, statistical evaluation are done automatically. The first results however must be revised, on the basis of our *a priori* knowledge about the sample.

In the first step, the macro loads the peaklist file and the PGAA library, which contains up to 25 of the strongest prompt-γ lines for each element, as well as the γ-lines attributed to the background radiation. For each line in the peak list, matches with $\left(\chi_E < 3\right)$ are assigned from the library, and the equivalent masses are calculated according to Eq. (6). In the next step, gamma lines are sorted by chemical elements, and the outliers are rejected by statistical tools. Finally, a **weighted average** of the mass and an overall uncertainty are calculated from the individual peaks. The statistical (or accidental systematic) uncertainty of the weighted mean is usually much smaller than if the analysis would have been done on the basis of only a single peak. Furthermore, a **quality factor** is calculated, too, that depends on the number of the identified peaks and their relative emission probabilities. The absence of the strongest lines strongly affects the quality number, while the absence of weak lines has little effect.

If the energies of certain peaks significantly deviate from the database value, or the individual masses do not agree with average mass, the given peak is discarded by the macro or by the analyst, i.e. it will not be used in further calculations, and the final mass and uncertainty values are recalculated. On a **result sheet**, the macro collects the "real" identified

11

components, and calculates their **concentrations** after background correction. The results are given in various units (atomic % and mass %).

	B	C	J	L	M	U	V	X	AA	AB	AD	AE	AF	AG	AH	AI	AJ	AL	AM	AN
1	meas. E (keV)	E unc	Rel. Int.	El.	No.	mcorr	*	dm%	<m>	<s>%	err%	dm/s	dE/s	chi^2 for m	chi^2 for E	P	f dec	-m (int)	interferences	
62	2885.24	0.5	8.1	P	17	0.00439		27									1	0	3397.369(SE) 3907.728(DE)	
63	841.013	0	100	S	1	0.10654	*	2.4	0.1055	2.1	1.5	0.40	0.00	0.30	1.04	1.00	1	0		
64	2379.61	0.1	59.9	S	2	0.10405	*	2.8				-0.50	1.45				1	0	3401.997(DE)	
65	5420.48	0.2	88.9	S	3	0.10221	*	3.6				-0.87	1.05				1	0	6441.812(DE)	
66	3220.53	0.1	35.8	S	4	0.10458	*	2.9				-0.31	1.34				1	0		
67	2930.67	0.1	23.9	S	5	0.10513	*	3.4				-0.11	0.74				1	0		
68	4869.47	0.2	18.7	S	6	0.10358	*	4.6				-0.40	1.38				1	0		
69	2753.18	0.1	7.96	S	7	0.10296	*	4.3				-0.56	0.90				1	0	3777.180(DE)	
70	3369.69	0.1	7.83	S	8	0.10522	*	4				-0.07	1.58				1	0		
71	1697.18	0.1	3.6	S	9	0.10256	*	7.6				-0.37	-0.17				1	0	2717.163(DE)	
72	4430.47	0.2	7.56	S	10	0.10378	*	4.1				-0.40	1.05				1	0	5452.440(DE)	
73	2216.63	0.1	3.46	S	11	0.10699	*	10				0.14	-0.18				1	0		
74	1472.36	0	2.5	S	12	0.1077	*	2.9				0.70	0.78				1	0	2496.896(DE)	
75	2490.13	0.1	3.61	S	13	0.10465	*	3				-0.28	1.05				1	0	3002.128(SE)	
76	3723.6	0.1	3.82	S	14	0.11159	*	4.9				1.16	1.64				1	0	4234.812(SE)	
77	1964.83	0.1	1.89	S	15	0.10561	*	10				0.01	-0.27				1	0	2987.394(DE)	

FIGURE 8. Part of the mass table from the EXCEL macro. * in the coloumn "V" means that the given peak is included in the mass calculation. The mass value in cell „AA63" gives the average mass, next to it, one can find the "internal error" (calculated from individual errors of mass values, applying error propagation) and the external error (experimental spread around the average). Columns „AE" and „AF" contain the normalised deviation of mass and energy values from the average (μ) $\left(\chi = \frac{x - \mu}{\sigma} \right)$, while in cell „AI63" one can find the quality factor for a given element.

ANALYTICAL PARAMETRES OF BUDAPEST PGAA SYSTEM

One chemical element is considered to be present in the sample, when at least its most intense peaks are identified in the spectrum. The peak search algorithm of HYPERMET-PC is able to identify a peak in the spectrum if its amplitude is greater than three times the standard deviation of background counts in its neighbouring channels. Supposing that the peak can be described with Gaussian curve, the peak area is: $N_P = \Gamma \delta \sqrt{\pi} = \Gamma \sqrt{\pi} W / 1.6551 \approx \Gamma \cdot W$. Due to the Poisson statistics the standard deviation of background (b) equals to $\sqrt{b}$. The amplitude of the minimum detectable peak is therefore $\Gamma = 3\sqrt{b}$, thus the **lower limit of detection** (m_{DL}, *Limit of Detection, LOD*) for one single element is:

$$m_{DL} = \frac{N_{P,DL}}{S \cdot t} \approx \frac{3 \cdot \sqrt{b} \cdot W(E_\gamma)}{S \cdot t} = \frac{3 \cdot M \cdot \sqrt{b} \cdot W(E_\gamma)}{N_A \cdot \Phi_0 \cdot \sigma_\gamma \, \varepsilon(E_\gamma) \cdot t} \tag{7}$$

where $N_{P,DL}$ is the minimum detectable peak area of an E_γ energy line, S is the analytical sensitivity (count rate originates from unit mass of a given element, cps/mg), W is the full width at half maximum (*FWHM*). The lower limit of detection depends on the background determined by the sample matrix, thus it can be different for different kinds of samples. Typical detection limits for the Budapest PGAA facility are shown on FIGURE 9. **Limit of quantification** (*Limit of Quantitation, LOQ*), in addition, depends on the tolerable uncertainty of the analytical results.
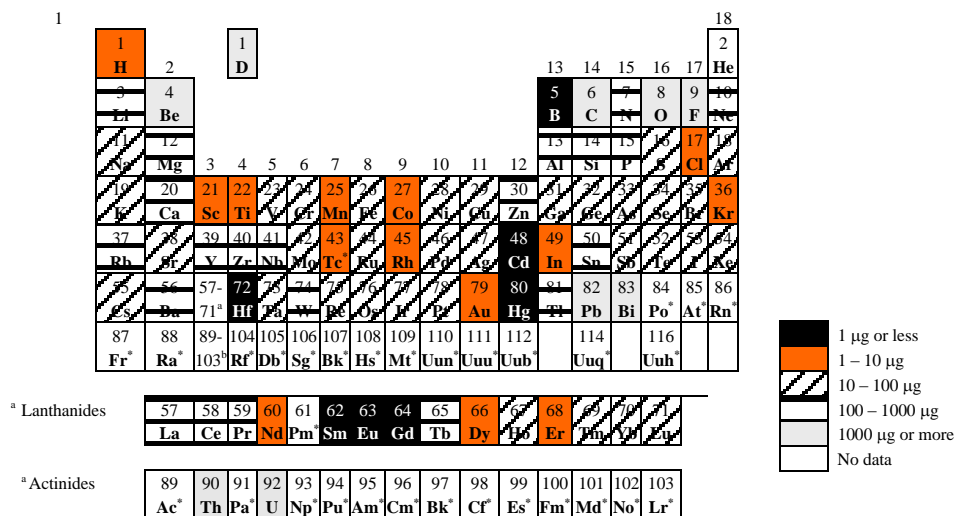
FIGURE 9. Lower limits of detection at the Budapest PGAA system.

The best conditions of detections and 30000 s acquisition times are assumed.

EXERCISES

1. Study the facility
2. Measure the "JB-3" basalt standard sample by PGAA. Identify the main components using the most intense peaks and the spectroscopic library.
3. Evaluate a background spectrum and identify background lines.
4. Evaluate the PGAA spectrum of the "JB-3" sample.
5. Compare the results to the certified concentrations and draw conclusions.
6. Calculate detection limits for Co, Cr, Eu trace elements.

LITERATURE

- László Szentmiklósi: *Time-dependent processes in Prompt gamma activation analysis*, Ph.D. thesis, Budapest University of Technology and Economics, Faculty of Chemical Engineering, Department of Physical Chemistry, 2006 (in Hungarian)

- Alfassi, Z.B., Chung, C., 1995, *Prompt Gamma Neutron Activation Analysis*, (Boca Raton: CRC Press).

- Molnár, G.L., 2004, Ed., *Handbook of Prompt Gamma Activation Analysis* (Dordrecht: Kluwer Academic Publishers).

Comment [K.Zs.3]: Ezek kellenek most?

APPENDICES

1. The peak shape function of Hypermet-PC

In mid-1970s PHILLIPS and MARLOW proposed a **semi-empirical peak shape function** which is either in its original formalism, or somewhat modified, is still implemented in several gamma spectroscopy software. (HYPERLAB; HYPERMET-PC). The value of the function in the jth channel of a region can be calculated as follows:

$$p(j) = \Gamma \cdot \left[e^{-\left(\frac{j-x_0}{\delta}\right)^2} + \frac{1}{2} A \cdot e^{\left(\frac{j-x_0}{\beta}\right)} \cdot \text{erfc}\left(\frac{\delta}{2\beta} + \frac{j-x_0}{\delta}\right) + \frac{1}{2} R \cdot e^{\left(\frac{x_0-j}{\rho}\right)} \cdot \text{erfc}\left(\frac{\delta}{2\rho} - \frac{j-x_0}{\delta}\right) \right], \quad (F1)$$

where $\text{erfc}(x) = 1 - \frac{2}{\sqrt{\pi}} \int_0^x e^{-t^2} dt$ is the complementer error function.

The first term of the (F1) peak shape is a **Gaussian** that represents the statistical fluctuation of the charge creation and the electronic noise of the signal processing. Its parameters are the position x_0, the amplitude Γ and the width δ (that is $\sqrt{2}\,\sigma$).

The second term is the so-called **Left Skew** to take into account the incomplete charge collection. In some cases, the detector measures lower energy than the photon energy that results in an exponential distribution. In a real spectrometer, this theoretical distribution is convolved with the above derived Gaussian, giving an Exponentially Modified Gaussian (EMG) function. It has a relative amplitude A and a skew parameter β; both are energy dependent.

In case of high count rate a distortion can be observed at the high-energy side of the peak due to the pile up effect. In order to deal with this, a **Right Skew** can be introduced. This is also an Exponentially Modified Gaussian with parameters R and ρ. Its use must be judged based on the quality of the electronics and the acquisition conditions. This component is missing from the HYPERMET-PC program. In short, the peak shape function is the sum of a Gaussian and one or two EMG functions, where the peak area is the sum of the areas of these components.

$$N_P = \Gamma \cdot \left[\delta \cdot \sqrt{\pi} + A \cdot \beta \cdot e^{\left(-\frac{\delta^2}{4 \cdot \beta^2}\right)} + R \cdot \rho \cdot e^{\left(-\frac{\delta^2}{4 \cdot \rho^2}\right)} \right] \quad (F2)$$

The model function comprises terms to describe the **background** features. This includes a **Step** function, being the convolution of a Heaviside function with the Gaussian. This describes the photons of original energy E_0 that were scattered in very narrow angle in the collimator or in the insensitive layer of the Ge crystal. The value of S is about $0.001 - 0.003$ times the peak area and increases with the gamma-ray energy. Under the escape peaks a reverse step can be observed, because one or both annihilation photons can deposit a small energy in the active volume before escaping from the crystal.

The other term of the background is the so-called **Tail**. This is yet another EMG function, but represents detector surface effects. Its amplitude (T) is about 0.1-0.01 times of the peak amplitude, just like its decay parameter (ν) is in this range of the peak width. It is mainly present only in case of low-energy but intense peaks.

$$b(j) = \Gamma \left[S \frac{1}{2} \text{erfc}\left(\frac{j-x_0}{\delta}\right) \right] + \Gamma \left[T\, e^{\frac{j-x_0}{\nu}} \frac{1}{2} \text{erfc}\left(\frac{j-x_0}{\delta} + \frac{\delta}{2\nu}\right) \right] \quad (F3)$$

The smooth baseline of the region is described with a **polynomial** up to second degree:

$$l(j) = a_0 + a_1 j + a_2 j^2 \quad (F4)$$

14

If there are m peaks in a R channel wide region, we set up the region to have smooth baseline at the two sides and we fit a function with maximum $n = 2m+11$ free variables. They are the positions and amplitudes for each peak, plus the two parameters (rel. amplitude and decay parameter) of the Skew, Tail and Right Skew, the rel. amplitude of the Step, the width parameter δ and the maximum three polynomial coefficients. The b and a_1, a_2 coefficients are optional. During a **weighted nonlinear least square fit**, we minimize the below defined χ^2 merit function:

$$\chi^2 = \frac{1}{R-n} \sum_{j=0}^{R} \frac{\left[y(j) - \left\{ l(j) + \sum_m \left[p_m(j) + b_m(j) \right] \right\} \right]^2}{y(j)} \to \min! \tag{F5}$$

In the optimum, the normalized χ^2 has an expectation value 1 and a standard deviation $\sqrt{\dfrac{2}{R-n}}$.

2. The NIPS-NORMA facility

The NIPS facility is located 1 m downstream of the PGAA facility at the end position of the neutron guide NV1. The Neutron-Induced Prompt gamma-ray Spectroscopy (NIPS)/Neutron Optics and Radiography for Material Analysis (NORMA) facility has been designed for a large variety of experiments involving nuclear reaction-induced prompt and delayed gamma radiations, including γ-γ-coincidences, large-sample PGAA, Prompt-Gamma Activation Imaging (PGAI) [4], as well as neutron radiography (NR) and tomography (NT).

The beam arrives through a flight tube of 4.0×4.0 cm^2 as free cross sectional area. If multiple detectors are to be placed close to the sample, a narrow aluminum tube with a $4 \times 4 \times 4$ cm^3 sample chamber is available. Alternatively a sample chamber with dimensions of $20 \times 20 \times 20$ cm^3 is available for large-sample PGAA and position-sensitive applications. It is made of AlMgSi alloy, and lined from inside with ^{6}Li-enriched polymer. By removing one or more side panels, larger objects up to 5 kg weight could also be analyzed (such as a sword, vase, stones, etc.). Samples can be loaded manually from the top, or placed onto an XYZω motorized sample stage with a travel distance of 200 mm and a guaranteed precision of 15 μm, which is introduced from the bottom. If custom devices are to be built into the beam, a short flight tube without a sample chamber is the proper choice.

An n-type coaxial HPGe detector (Canberra GR 2318/S) equipped with a Scionix BGO Compton suppressor is used for the routine prompt gamma measurements. This latter can accommodate HPGe detectors with larger crystals (up to end cap diameter of 76 mm). The passive shielding is made of standard lead bricks.

A digital signal processor combined with an Ethernet-based multichannel analyzer module (Canberra AIM 556B) collects the counts. Alternatively, a four-channel, all-digital XIA Pixie 4 spectrometer can also be used.
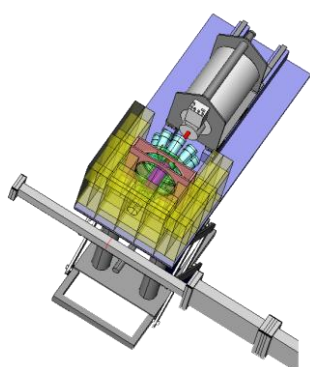
The NORMA setup also comprises an imaging system. It consists of a 100 μm thick ^{6}Li/ZnS scintillator, a quartz mirror with Al layer and a cooled, black-and-white, back illuminated Andor iKon-M CCD camera with 1024×1024 pixels and 16-bit pixel depth, mounted in a light tight aluminum housing. The custom optics projects a 48.6×48.6 mm^2 area (in which the beam spot is about 40×40 mm^2) onto the 13.3×13.3 mm^2 sensitive surface of the CCD chip. The spatial resolution of the imaging system changes linearly between 230-660 μm according to the 1.5-100.5 mm distance from the scintillator screen, respectively. The measured collimation ratio, L/D characteristic to the neutron beam's divergence, was found to be 233. The specifications of the facility are listed in Table 3.

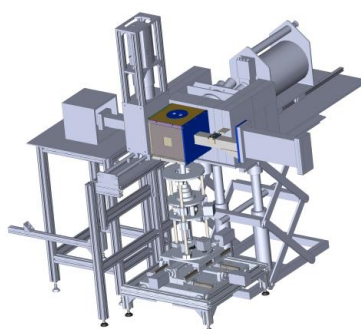*Table 3. Specifications of NIPS/NORMA facility*

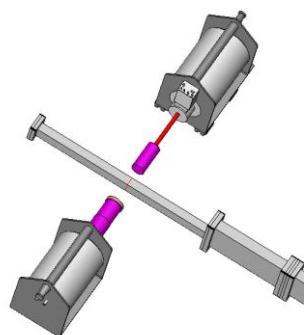| Beam tube:	NV1 guide, end position
Distance from guide end:	2.6 m
Beam cross section for imaging and PGAA/PGAI:	Any rectangular shape with arbitrary side lengths up to 4.0 cm
Thermal-equivalent flux at target:	≈$2.7 \times 10^7 \cdot$cm^{-2}s^{-1}
Vacuum in target chamber:	Not available
Form of target at room temperature:	Solid, powder, liquid; gas in a pressurized container
Target packing at atmospheric pressure:	sealed FEP Teflon bag or vial
Sample chamber dimensions:	$4 \times 4 \times 4$ cm^3/$20 \times 20 \times 20$ cm^3

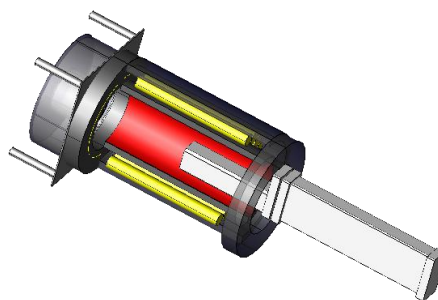|	
Distance from target to detector window:	minimum 25 mm, typical 280 mm
γ-ray detector	n-type coax. HPGe, with BGO shield
HPGe window:	Al, 0.5 mm
Relative efficiency:	23% at 1332 keV (^{60}Co)
FWHM:	2.2 keV at 1332 keV (^{60}Co)
Compton-suppression factor	≈3.5 (1332 keV) to ≈30 (7000 keV)

A) element analysis of small samples

B) large-sample PGAA/position-sensitive element analysis with radiography-driven PGAA or PGAI (NORMA)

C) coincidence measurements with multiple HPGe detectors

D) experiments with a custom equipment (the figure illustrates an in-beam neutron coincidence counting setup)

Figure 4. Possible configurations of the NIPS/NORMA experimental station. The beam arrives from the lower-right corner of the images.

<u>Data acquisition and data processing</u>

The radiography images taken at NORMA require several steps of data treatment. The spatial inhomogeneity of the beam and the thermal noise of the camera should be removed. These are called 'beam image correction' and 'dark image correction', respectively. In tomography, the goal is to determine a measure of the interaction probability between the material and the neutron as a function of spatial coordinates. This quantity delivers the structural information about the interior of the sample. The reconstruction codes, such as the OCTOPUS reconstruction software, apply the inverse Radon-transformation and filtered back projection algorithms. The visualization of the dataset in 3D space (volume rendering) is carried out using VGStudio 2.1